

Supramolecular Design of Cellulose Hydrogel Beads

Poonam Trivedi¹, Jens Schaller², Jan Gustafsson¹ and Pedro Fardim^{1,3*}

¹Laboratory of Fibre and Cellulose Technology, Åbo Akademi University, Tuomiokirkontori 3, 20500 Turku, Finland

²Thuringian Institute of Textile and Plastic Research, Breitscheidstraße 97, 07407 Rudolstadt, Germany

³Department of Chemical Engineering, KU Leuven, Celestijnenlaan 200F bus 2424 B-3001 Leuven, Belgium

Received October 21, 2016; Accepted April 23, 2017

ABSTRACT: In the present study, we report the supramolecular design of cellulose-sulfonate hydrogel beads by blending water soluble sodium cellulose ethyl sulfonate (CES) with the pretreated cellulose in sodium hydroxide-urea-water solvent system at $-6\text{ }^{\circ}\text{C}$ followed by coagulation in the 2M sulfuric acid system. The increasing of CES amount from 10% to 90% had a substantial effect on the viscosity and storage (G') and loss (G'') moduli of the blended solutions. The CES concentration up to 50% in blends led to the formation of physically stable hydrogels after coagulation in acidic medium at pH-1 and showed the retention of nearly the same CES concentration at pH-6 after continuous water washings. The increased sulfonate content also enhanced the water holding capacity and internal porosity of the beads. Both ATR-FTIR and Raman spectrometry were used for the qualitative determination of sulfonate groups and SEM-EDX was used for the quantitative estimation in dried beads. In this research, we have established a correlation between the presence of anionic charge in the polysaccharide blend and stability of the prepared hydrogel beads. Hence our research provides a systematic methodology to design functional, highly porous cellulose hydrogels having the potential to be tested further in biomedical and healthcare applications.

KEYWORDS: Blending, hydrogen bonding, anionic groups, hydrogel, beads, coagulation

1 INTRODUCTION

Polysaccharides of natural origin are one of the most diverse and well-structured polymers on earth. The variance in the backbone structure and functional groups impart their applications in versatile areas of medicine and healthcare. For example, cellulose, agarose, dextran, and starch are the polysaccharides bearing hydroxyl functional groups. Similarly, alginate and hyaluronan are weak anionic polymers with carboxylic moieties, carrageenans and heparin are strong anionic polysaccharides with sulfonate groups and chitosan, cationic polymer has amino functional groups [1].

Cellulose has numerous hydroxyl groups available for the chemical modifications like oxidation, esterification, etherification and amination in appropriate solvents such as DMA-LiCl, NMMO-H₂O and ionic liquids [2]. The functional group introduced, and the degree of substitution plays a decisive role in polymer properties like solubility, rheological behavior, and

processing into the final desired product. For example, cellulose ethers used as thickeners in paints, food, and personal care areas are soluble in organic solvents at selective DS only, in contrast to cellulose esters [3]. Cellulose sulfate with DS range of 0.08–0.16 is water insoluble while 0.36–0.58 is water soluble [4]. The sulfated polysaccharides are known to have antiviral property, which is also dependent upon the degree of sulfation and molecular mass [5].

Polysaccharides bearing sulfate functional groups are of practical interest. The sulfated polymer heparin is an anticoagulant and has been used to increase the biocompatibility of several materials as a coating agent [6]. Heparin affinity beads have been used for the isolation and purification of extracellular vesicles [7]. The cellulose sulfate beads with low sulfate content have been used during the primary fractionation procedure for influenza vaccine production [8]. Another application of the beads is in the downstream processing of Vero cell-derived human influenza A virus (H1N1) grown in serum-free medium and development of Vero cell-derived inactivated Japanese encephalitis vaccine [9, 10]. These beads have also shown an affinity towards antithrombin III, blood coagulation factor, and several enzymes as well as viruses [11]. Cellulose

*Corresponding author: pfardim@abo.fi

DOI: 10.7569/JRM.2017.634143



sulfate has been studied for the preparation of poly-electrolyte capsules for the encapsulation of enzymes, drugs, and adhesion of mouse fibroblasts [12].

Functional polysaccharides can be used to prepare advanced materials by employing a polymer blending approach for wound healing, drug delivery, and tissue engineering applications [13]. The blending of polymers has the potential of self-assembly due to the presence of intermolecular interactions [14]. These intermolecular or supramolecular interactions can be used to design materials with desired properties such as high porosity and hydrophilicity. In one study [15], enhanced thermal processability of cellulose acetate was achieved by blending with synthetic polymer poly(N-vinyl pyrrolidone) while blending of cellulose propionate with poly(N-vinyl pyrrolidone-co-methyl methacrylate) improved thermochemical and optical properties of the polymer [16]. The polymer blending is a versatile and economical mode of preparing new materials which can satisfy the complex performance demands [17]. The desired shaping of polysaccharide solution also requires knowledge of rheological properties under certain conditions. The rheological parameters, e.g., viscosity, storage and loss moduli, of the blend provide significant information related to the processing of the product. The rheology of polymers is directly dependent upon the functional group, the degree of substitution, counter ion, molecular weight and solvent polarity. These parameters are the reason for hydrogen bonding, van der Waals forces, electrostatic attraction and repulsion in the systems [18]. For example, carboxymethylcellulose, which is a derivative of cellulose, is water soluble and shows different rheological behavior with increasing concentrations [19, 20].

In the present study, we have used supramolecular design to fabricate cellulose-sulfonate hydrogel beads by blending water soluble cellulose derivative (CES) with HyCelSolv pretreated cellulose in 7% NaOH–12% urea-water solvent system. The sulfonated hydrogel beads obtained have shown higher hydrophilicity and porosity than conventional cellulose beads, and their potential future application can be further explored in the areas related to tissue engineering, healthcare and pharmaceutical applications.

2 EXPERIMENTAL

2.1 Materials and Methods

Enoalfa cellulose dissolving pulp with alpha cellulose content > 93.5% was provided by Enocell pulp mill, Finland, sodium cellulose ethyl sulfonate (CES) was provided by TITK Germany, and sodium hydroxide (NaOH, 97%) from Fluka. Urea ($\text{CO}(\text{NH}_2)_2$, 99.5%),

sulfuric acid (H_2SO_4 , 98%) and hydrochloric acid (HCl, 37%) were purchased from Merck. Ethanol (92%) and sodium sulfate (Na_2SO_4 , 98%) were from Sigma-Aldrich, and deionized water from the Milli-Q system was filtered through 0.2 μm filters.

2.2 Synthesis of Sodium Cellulose Ethyl Sulfonate

A detailed procedure of the synthesis of sodium cellulose ethyl sulfonate is described here. First 8.1 g air-dried cellulose (spruce sulphite pulp, $\text{DP}_{\text{Cuoxam}}$ 450) was added to 100 ml 2-propanol, followed by a solution of 3.0 g NaOH and 3.2 g sodium vinyl sulfonate while stirring. After 10 min the reaction mixture was heated at 80 °C. After 1 h a solution of 3.2 g sodium vinyl sulfonate in 10 ml water was added and stirred for 3 h at 80 °C. After cooling down to room temperature, the product was filtered off and neutralized with acetic acid. Finally the cellulose derivative was washed with 80% 2-propanol to remove by-products. The obtained derivative has 0.48 degree of substitution.

2.3 Preparation of Enoalfa HyCellSolv Cellulose Pulp

A HyCellSolv pretreatment of Enoalfa pulp was performed according to the procedure developed in our laboratory [21]. In a 200 mL borosilicate vessel, 100 mL ethanol was mixed with 4 mL HCl (37%) and heated at 75 °C. The pulp was added to the ethanol-acid mixture and heated for 2 h. After cooling, the solvent was decanted and the pulp washed with excess water. The pulp was dried in an oven at 60 °C. Capillary viscosity measurements were done following ISO 5351 protocol to calculate the degree of polymerization of pretreated pulp. The calculated degree of polymerization of the pretreated pulp was 170.

2.4 Polymer Blending Studies

The polysaccharide blends were prepared by mixing various ratios of CES and Enoalfa HyCellSolv cellulose pulp in 7% NaOH–12% urea-water solvent system. Detailed information about blending ratio is given in Table 1. A 5% (w/w) final polysaccharide concentration was maintained in all blended solutions with a total weight of 10 g of each solution. In 30 mL glass vials, the pre-calculated amount of both the polysaccharides were dispersed in 7% NaOH–12% urea-water system for 30 min followed by dissolution at –6 °C for 1 h. All blends were stored at 0 °C before dropping into the 2M sulfuric acid, the coagulation medium.

Table 1 The ratio of CES and Enoalfa HyCellSolv.

S. No	Ratio of *sodium cellulose ethylsulfonate/ Enoalfa HyCellSolv
1	*0/100
2	*10/90
3	*30/70
5	*50/50
6	*70/30
7	*90/10
8	*100/0

2.5 Coagulation of Polymer Blends into Hydrogel Beads

The immersion precipitation technique was used to prepare CES blended hydrogel beads. In a 20 mL syringe, the polysaccharide blends were filled, and droplets were extruded through a needle with a diameter of 0.4 mm. In each case, the distance between the needle tip and the coagulating solvent was kept to 2 cm. To select the optimal coagulating solvent system, initially the *50/50 polymer ratio blend was dropped into the following coagulating solvents: 2M HCl, a mixture of 2 M HCl–ethanol (50:50), 50% aqueous sodium sulfate and 2M sulfuric acid. The process of coagulation of the droplets to solid beads was followed up. The most suitable coagulation medium proved to be 2M sulfuric acid and was used further as a coagulating medium. Finally, the beads were washed with tap water followed by washing with deionized water. To study the effect of increasing CES concentration on the shape and size, the beads were scanned and processed into binary images using ImageJ software.

2.6 Rheological Studies

Oscillatory and steady state rheological experiments were performed to measure the viscosity and storage and loss moduli of 5% (w/w) polymeric blends in a solution of 7% NaOH–12% urea–water system at 10 °C and 25 °C ± 0.1. An Anton Paar Physica MCR 300 rotational rheometer with double gap cylinder module DG 26.7 with attached temperature controlling TEZ 150P thermostat possessing external water circulation was used. Each blend was stored at 0 °C (±1) before measurements and 3 mL solutions were used for all measurements. For the oscillatory measurements frequency varied from 0.5 to 500 Hz, and for viscosity measurements, a steady shear rate was increased from 0.1 to 1000 s⁻¹. RheoPlus 32 software was used to summarize the results.

2.6.1 Water Holding Capacity

The effect of increasing sulfonate content on the water holding capacity was measured by removing excess surface water from the hydrogel bead on filter paper; 20 wet beads from each blend were weighed in triplicate sets and dried in an oven at 60 °C ± 1 for 48 h and cooled in a desiccator until constant weight was achieved. The water holding capacity (WHC) in percentage was determined using the following equation:

$$\text{WHC (\%)} = (W - W_d) / W_d \times 100 \quad (1)$$

where W is the total weight of wet beads and W_d is the total weight of dry beads.

2.6.2 FTIR and Raman Analysis

A Nicolet iS50 FT-IR spectrometer with Raman module from Thermo Scientific was used for spectrometric measurements. The FTIR spectra were collected using a tungsten-halogen source and DLaTGS-KBr detector splitter set up with 4.00 cm⁻¹ resolution and 128 scans. Raman spectra were collected using a diode laser with 0.5-W power. The detector was InGaAs with CaF₂ splitter; resolution 8.0 cm⁻¹ and number of scans was 11000.

2.6.3 Scanning Electron Microscopy-Energy Dispersive X-ray Analysis (SEM-EDX)

Surface-core morphology and sulphur weight percentage analysis of CES beads were performed with a LEO Gemini 1530 scanning electron microscope. The Thermo Scientific Ultra Silicon Drift Detector (SDD) was equipped with secondary electron backscattered electron and in-lens detector. Surface dried hydrogel beads were frozen in liquid nitrogen and freeze-dried under vacuum to maintain the pore structure. The dried beads were cut into cross sections coated with carbon and analyzed. The magnification of image corresponds to a Polaroid 545 print with the image size of 8.9 × 11.4 cm.

3 RESULTS AND DISCUSSION

3.1 Effect of Increasing CES Concentration on Coagulation and Properties of Hydrogel Beads

The effect of increasing anionic cellulose concentration in hydrogel beads was studied. The phase separation phenomenon which involves ion exchange between OH⁻ and H⁺ ions is the mechanism of alkali cellulose coagulation in the acidic medium [22]. The preliminary investigation of solvent systems for the

coagulation of homogeneously blended CES-Enoalfa HyCellSolv solution in bead shows that the performance of 2M sulfuric acid precedes over 2M HCl, 2M HCl-ethanol (50:50) and aqueous 50% sodium sulfate solutions. Dropping of *50/50 blend resulted in spherical hydrogel beads in 2M sulfuric acid, while flattened, deformed disc-shaped structures were coagulated in 2M HCl and 2M HCl-ethanol solvent systems. The flattening and irregular structure formation could be due to the surface tension effects of the coagulation media. In aqueous 50% sodium sulfate solution, thin films of polymer were observed after 2 h. This behavior could be related to the slow process of coagulation in a salt solution [23].

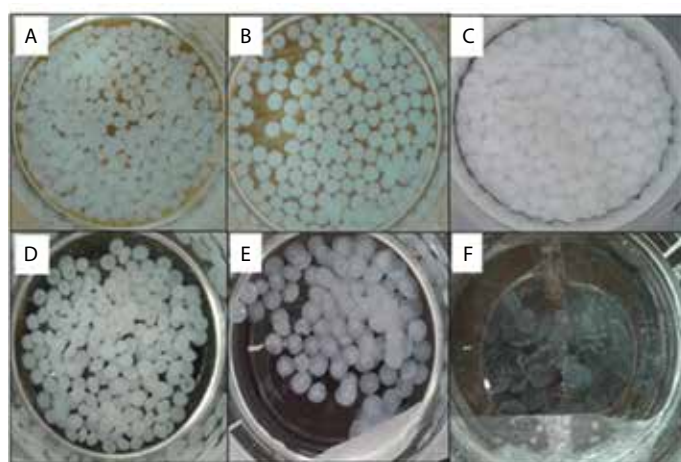
The cellulose blends with CES/Enoalfa HyCellSolv ratio ranging from *10/90 to *90/10 coagulated out while minor precipitation of 100% CES is also visible, as shown in Figure 1a. The slight precipitation of CES at pH ~1 could be due to the ion exchange leading to the protonation of sulfonate ions, ultimately resulting in sulfonic acid. A variation in the shape of the beads from spherical to flattened was also observed with increasing CES concentration after coagulation, even though the distance between the needle tip and the coagulating medium was kept constant (2 cm) in each case. These observations show that the Enoalfa HyCellSolv pulp plays a crucial role in maintaining the contour and acts as a support matrix providing structural stability to the hydrogel beads. The processed binary images of beads displayed a correlation between increasing CES concentration in the blend and the average surface area of hydrogel beads. The *0/100 beads had an average size of 6 mm, which

increased up to 11.7 mm for the *70/30 beads, as shown in Figure 1b. The increase in average size of the beads is related to the flattening of beads after contact with the acidic medium. The measured viscosity of *0/100 and *70/30 beads are approximately 0.9 and 0.7 at the shear rate 0.1 (s^{-1}) respectively. The lowered viscosity of the blends could be the possible reason for beads flattening with increasing CES concentration in the blends.

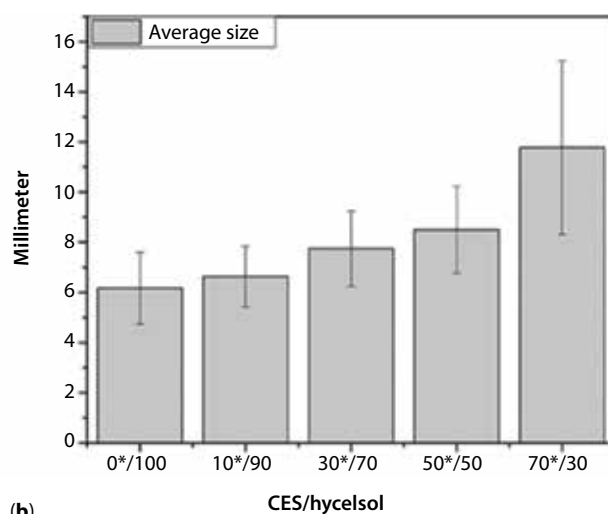
The *0/100 hydrogel beads show 93.7% water holding capacity, the *10/90 ratio 95% water holding capacity and *50/50 ratio 97% water holding capacity, as visible in Figure 2. The increase in water holding capacity can be directly related to rising sulfonate content and hence the surface charge of the beads, favorably absorbing an increasing amount of water. The SEM-EDX measured sulphur content of CES to be 8.75% by weight and in *10/90, *30/70 and *50/50 beads the sulphur content was 1.1%, 2.8% and 4.3% (± 0.25), respectively. The beads from *10/90 up to *50/50 ratio were stable at pH 6, while notable scaling

Table 2 Elemental composition of CES and dried cellulose sulfonate beads.

%CES	C (wt.%)	O (wt.%)	S (wt.%)	Na (wt.%)
CES	31.785	52.09	8.75	7.375
*0/100	41.18	58.82	0	0
*10/90	40.95	57.45	1.14	0.45
*30/70	39.61	56.76	2.89	0.74
*50/50	40	54.52	4.38	0.85



(a)



(b)

Figure 1 (a) Cellulose beads with increasing *cellulose ethyl sulfonate concentration: A) *10/90, B) *30/70, C) *50/50, D) *70/30, E) *90/10, F) *100/0. (b) Average increase in the size of beads.

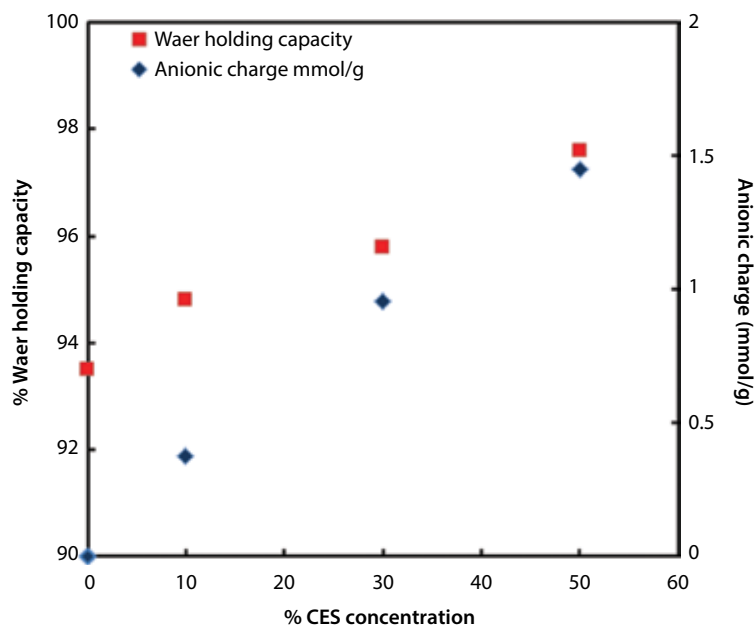


Figure 2 Correlation between the increasing anionic charge (mmol/g) with increasing % CES concentration and water holding capacity of the sulfonated cellulose beads.

is observed for beads with higher CES concentration. This behavior could be due to increased CES concentration, which in turn resulted in increased anionic charge content in the beads. Consequently, the increased ionic repulsion interactions due to ionized sulfonate groups led to destabilized structures at neutral pH [24].

3.2 Effect of Sulfonated Cellulose on the Rheological Behavior of Blends

Rheological studies of 5% (w/w) solutions of polymer blends were performed to understand the effect of increasing sulfonate content on viscosity and storage and loss moduli with varying shear rate in blends. Additionally, the effect of sulfonate content in the beads on their physical properties, e.g., shape, stability, and porosity, is due to the rheological behavior of the polymer solutions. A 5% polymer solution of CES and Enoalfa-pretreated cellulose in 7% NaOH–12% urea-water formed viscoelastic solutions which displayed an apparent frequency and temperature-dependent storage (G') and loss moduli (G''), as shown in Figure 3a. The storage modulus of CES solution at 10 °C was comparatively higher than at 25 °C, which is typical for charged polymers that disperse well in aqueous solutions. While in the case of Enoalfa HyCellSolv pulp no characteristic temperature dependence variation was observed since NaOH-urea solvents are not strong solvents for dispersing dissolving pulps with

low surface charge. A continuous increase in (G') and (G'') was observed with increasing frequencies. Thus, a predominance of viscous behavior over the elastic one in both the polymer solutions at 5% polymer concentration is obvious. Interestingly, HyCellSolv pulp displayed leveling off for (G') within the frequency range of 10 to 100 Hz, which CES did not reveal. The leveling off behavior could be assumed from the loss of elasticity with the increasing frequency due to coiling or entanglement of the polymer [25]. The aqueous-based NaOH-urea solvent is not favourably interacting with Enoalfa HyCellSolv pulp, due to the low surface charge. Consequently, the Enoalfa HyCellSolv cellulose polymers are less stretched out in the solvent but suggested to be more coiled compared to the CES polymers. The presumed coiled polymer structure cannot increase its elastic behavior above a certain frequency range. On the other hand, the charge-driven interaction between CES and NaOH-urea solvent leads to a more stretched out polymer structure and hence continuous increase of elastic modulus (G') in the frequency range investigated.

The similar behavior is apparent from the steady shear-rate-dependent viscosity measurements in Figure 3b. The 5% CES has a lower viscosity at low shear rates than Enoalfa pulp solution at both the temperatures. At constant temperature, there is a cross-over shear rate at around 5 s⁻¹. The lowered viscosity of CES in comparison with Enoalfa HyCellSolv pulp could be due to the higher water soluble nature, ionic

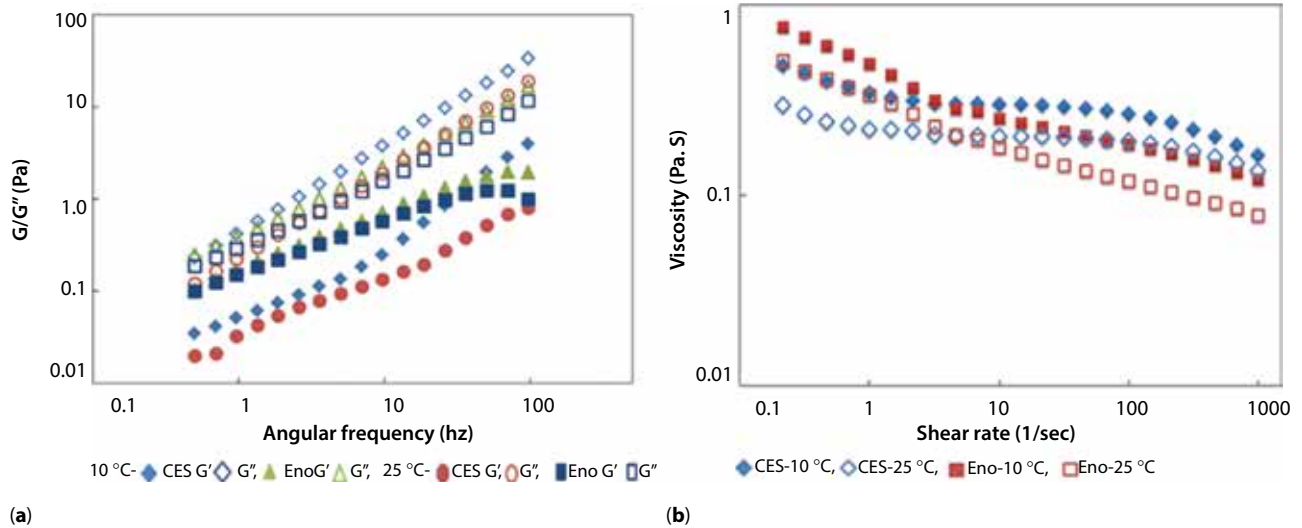


Figure 3 (a) Variation in the storage (G') and loss (G'') moduli with increasing angular frequency (Hz) and (b) Viscosity vs. Shear rate of CES and Enoalfa HyCellSolv at 10 °C and 25 °C.

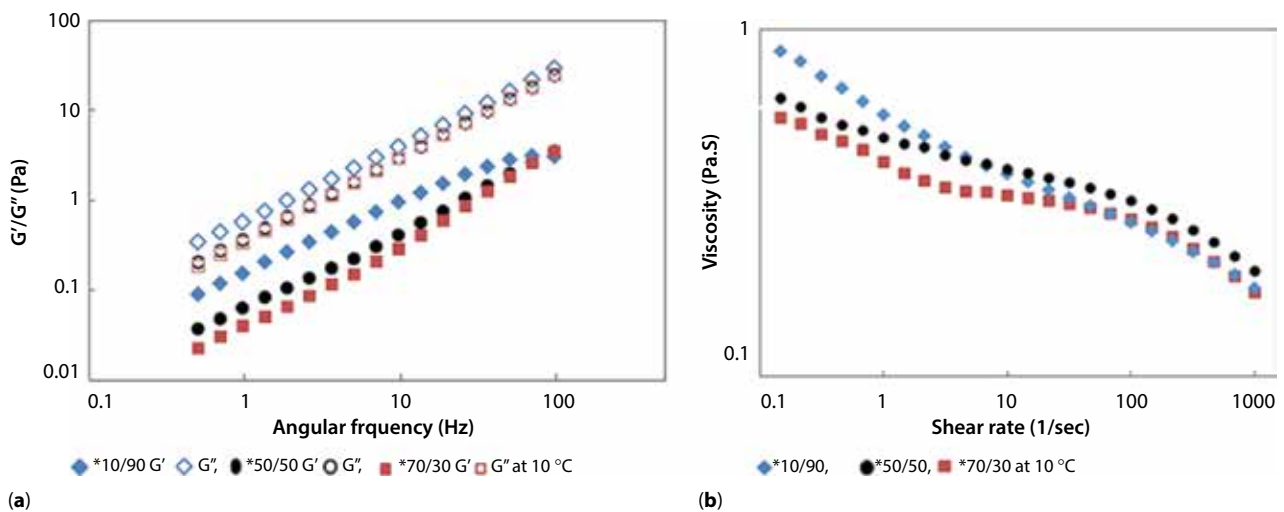


Figure 4 (a) Storage (G') and loss (G'') moduli and (b) Viscosity vs. Shear rate of various blends of CES:Enoalfa at 10 °C.

character and weaker inter- and intramolecular hydrogen bonding. Both the polymers displayed lower viscosity at 25 °C than at 10 °C in the studied polymer concentration. Both the polymeric solutions show a non-Newtonian behavior, but CES solution showed a plateau in the shear rate range of 10–100 reciprocal seconds and further viscosity decrease at shear rates above 100 s^{-1} .

The predominant interactions present in polymeric blends are hydrogen bonding, van der Waals forces and ionic interactions.

To prepare stable blends, polymeric associations or repulsions, polymer-solvent interactions play a very critical role [26]. To get an insight into the flow and

stability properties of polymeric blends of CES and Enoalfa pulp, the oscillatory and shear rheology of the blends were investigated. The (G') of *10/90 (CES/HyCellSolv) blend is comparatively higher than *50/50 and *70/30 blends at 10 °C in each blend in Figure 4a. The plateau of (G') at increasing frequency from 50–100 Hz is only visible for *10/90 blend, due to the high content of HyCellSolv. Increasing the concentration of CES for the other blends increased the average surface charge of the polymers and hence could lead to polymers with less coiling or entanglement [25] due to increased electrostatic repulsion between the polymers and increased favorable interaction of the polymers with the solvent. The loss modulus (G'') was, as

expected from Figure 3a, always greater than the (G') at 10 °C for each blend, as is seen in Figure 4a. The viscosity data of blends in Figure 4b showed that *10/90 solution had a slightly higher viscosity closer to one at a low shear rate in comparison to *50/50 and *70/30 blends. At the high shear rate, there was not a clear difference between the blends. At the low shear rate, the observed higher viscosities could be correlated to higher intermolecular associations in polymeric sub-units, while at high shear rate, shear thinning was predominant due to more top intramolecular interactions and elongation of polymeric chains. The reduction in viscosity could be due to the electrostatic repulsion which leads to disentanglement and loosening of the network structure [27].

Hence, from the rheological studies it was confirmed that increasing ionic polymer concentration in blended solutions resulted in lowered viscosity at low shear rate and a storage modulus at a low angular frequency, which could be the reason for beads flattening with increasing CES concentrations.

3.2.1 Spectroscopic Analysis

The ATR-FTIR and Raman spectrometric scanning of air dried beads in the range of 4000–500 cm^{-1} confirmed the presence of sulfonate functional groups in the beads. Here we have presented an extended spectral range from 1600–500 cm^{-1} , which provides significant information about sulfonate groups. The FTIR spectrum of beads with increasing sulfonate content shows distinct variation in the region of 1100–1400 cm^{-1} ,

which is attributed to the SO_2 in-phase, out-of-phase and SO_3 in-phase stretching vibrations in Figure 5a. The characteristic peak due to S-O stretching is also visible in the region 750–780 cm^{-1} [28]. The presence of all the characteristic peaks of sulfonate functional group confirmed the blending and retention of sulfonated ethyl cellulose in the hydrogel beads. The Raman data also confirms the presence of sulfonate groups in the beads in Figure 5b. A prominent peak at around 1100 cm^{-1} is present, which is due to the SO_2 out-of-phase stretching. The FTIR and Raman results prove the incorporation and retention of sulfonated cellulose in the hydrogel beads.

3.3 Effect of Coagulation Mechanism on Surface and Core Morphology of Hydrogel Beads

A variation in the architecture of beads with increasing CES concentration is noticeably visible in Figure 6a–d. The overall internal structure of the bead prepared from Enoalfa HyCellSolv cellulose solution displays zones in the cross section of the bead in Figure 6a. The outer layer is the surface skin followed by loosely oriented network structure and in the center is the compact area. The formation of layers could be related to the continuous coagulation process and the ion exchange during phase separation [29]. As the cellulose solution droplet comes in contact with the acidic medium, instant coagulation occurs due to the fast exchange of ions between alkaline cellulose solution

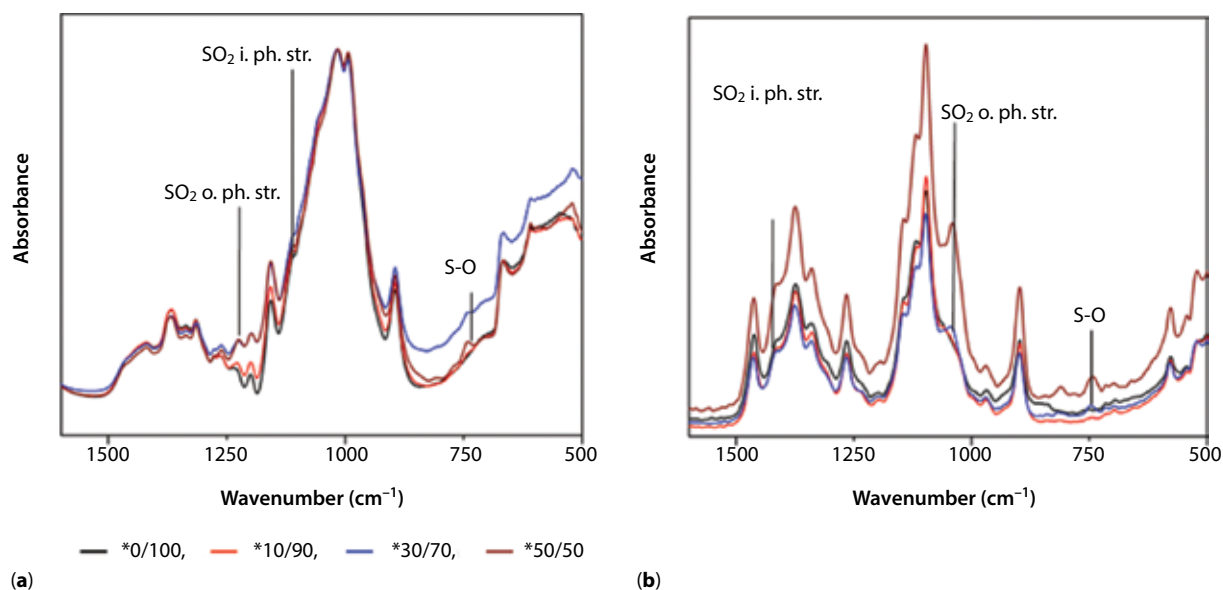


Figure 5 (a) Attenuated total reflectance-Fourier transform infrared (ATR-FTIR) and (b) Raman spectra of sulfonated cellulose beads with increasing sulfonate content.

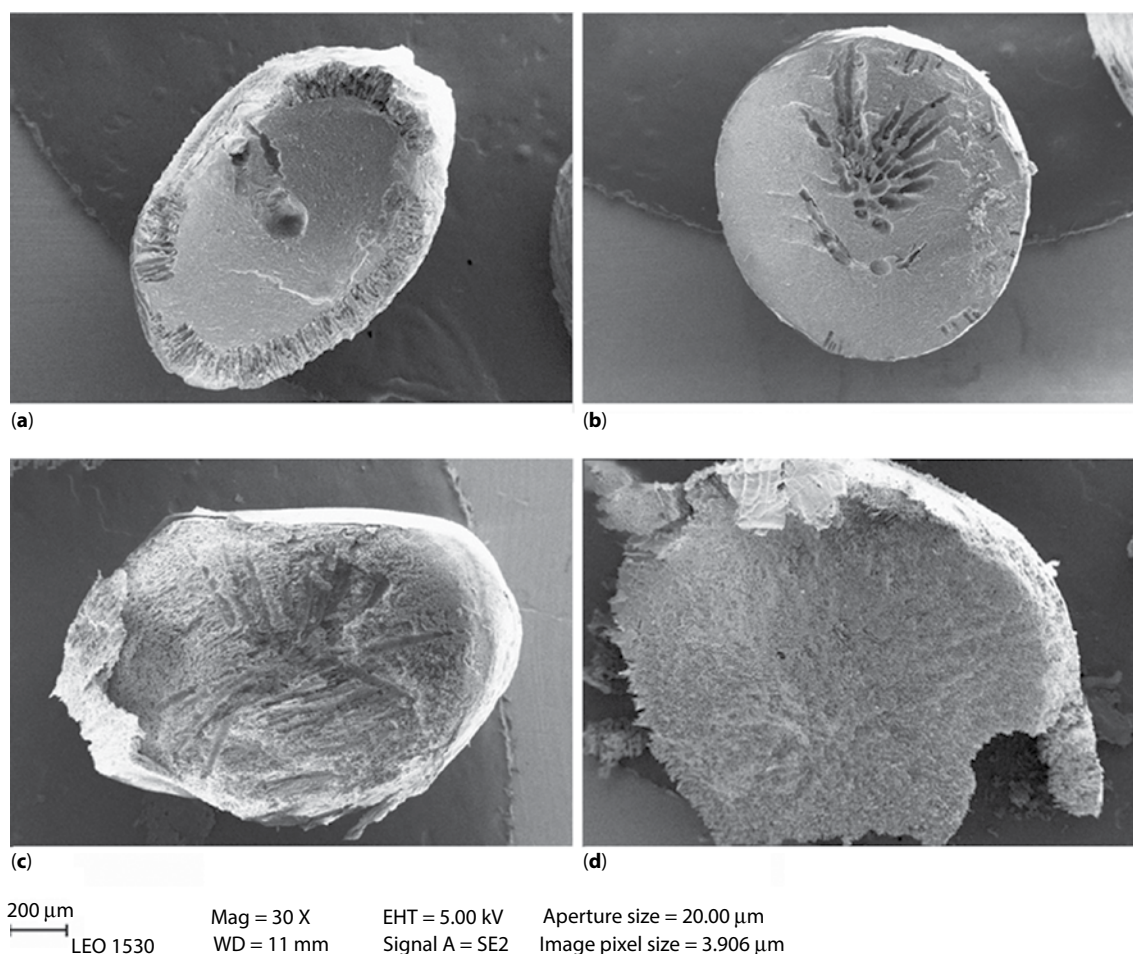


Figure 6 (a–d) Cross-section images of *0/100, *10/90, *30/70, and *50/50 CES/Enoalfa-HyCellSolv freeze-dried hydrogel beads, respectively.

and acidic medium, leading to the formation of an outer skin. The rate of exchange of ions is initially fast, resulting in the formation of the loose network, and when the system achieved equilibrium based on diffusion, the ion exchange process is slowed down, forming a compact network structure in the center. While in the case of the CES blended beads shown in Figure 6b–d, only two zones are observed, namely the surface skin and inside a compact region. The reason for this could be the slower ion exchange rate between sodium ion attached to sulfonate groups and the acidic protons.

The higher magnification images of surface skin show an increased smoothness and inside porosity with increasing CES concentration in the hydrogel beads, as visible in Figure 7a–d and 7e–h. The *0/100 and *10/90 beads have a more closed network structure in comparison to the *30/70 and *50/50 beads. This observation is related to the high concentration of Enoalfa HyCellSolv cellulose in the *0/100 and *10/90

blends. In 7% NaOH-12% urea, the aqueous solution of the HyCellSolv pulp is supposed to be coiled due to weak solvation and has stronger cohesive forces than the CES polymers in the same solvent. Hence, Enoalfa HyCellSolv cellulose polymers approach each other in the NaOH-urea solvent, and during coagulation of the NaOH-urea solution droplets containing these polymer blends in acid, the rapid coagulation process produces dense ultrastructures.

Furthermore, increasing concentration of the sulfonated CES polymer in the *30/70 and *50/50 blends increased the average surface charge of the polymer blend in NaOH-urea aqueous solution. Consequently, the increased average surface charge increased the solubility and dispersibility of the polymers and the electrostatic repulsion between the polymers, resulting in different rheological behavior of the polymer blends in Figure 4. Coagulation of *30/70 and *50/50 blends with well-separated polymers led to more porous ultrastructures. Additionally, a high content

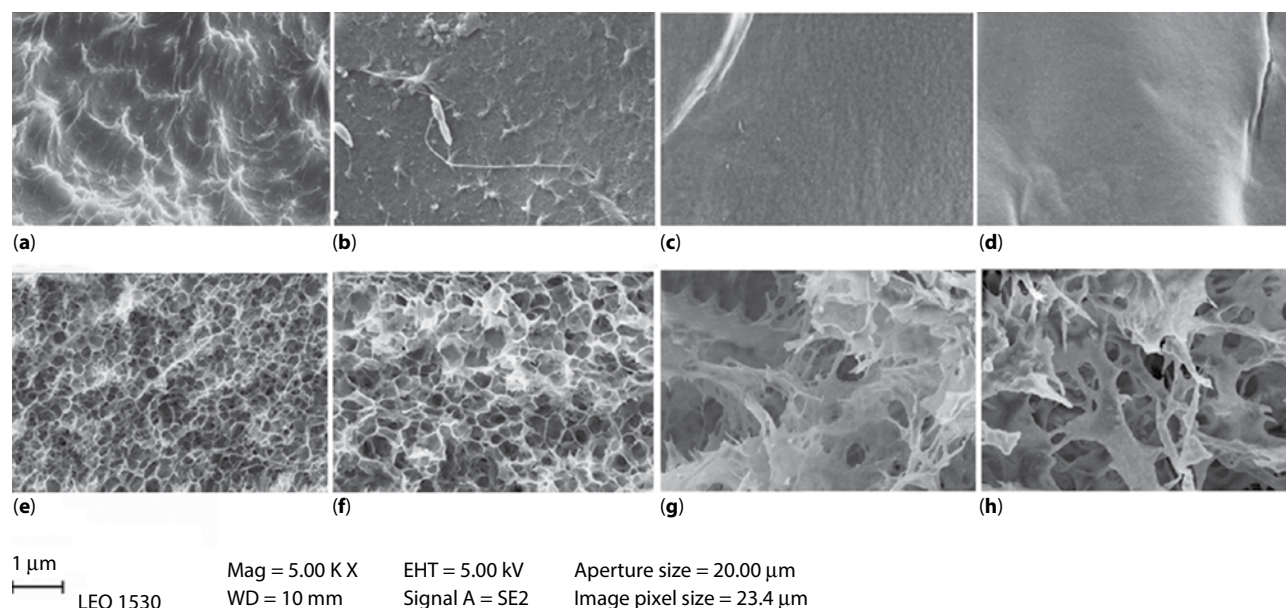


Figure 7 (a–d) surface and (e–h) internal morphology of *0/100, *10/90, *30/70, and *50/50 CES/Enoalfa-HyCellSolv freeze-dried hydrogel beads, respectively.

of CES resulted in the higher water holding capacity due to the charged groups which also controlled the porous structure in the beads.

4 CONCLUSION

The supramolecular properties of CES polymer and HyCelSolv pulp are utilized to design anionic hydrogel beads using blending of the biopolymers in sodium hydroxide–urea water solvent system. The CES polymer efficiently disperses and solubilizes in the solvent system due to the presence of charge and blends homogeneously with the HyCelSolv pretreated cellulose. A temperature-dependent variation in rheological properties of the individual polymer solutions is also observed. The polymer blends with increasing CES ratio have shown lower viscosity and storage moduli (G'). The extrusion and coagulation of blends in 2M sulfuric acid lead to the formation of hydrogel beads. The *50/50 beads have higher average surface area and water holding capacity than *10/90 beads. The morphological characterization of beads also shows higher surface smoothness and internal porosity in the case of *50/50 than in *10/90. In hydrogel beads, Enoalfa HyCelSolv pulp acts as support matrix to retain CES polymer by hydrogen bonding and van der Waals interactions. Hence, we postulate that the blending of anionic cellulose with low DP cellulose and coagulation in the acidic medium will lead to the formation of physical hydrogels with incorporated charge, higher water holding capacity and porosity.

These hydrogel beads can be further explored for potential application in biomedical and healthcare areas.

ACKNOWLEDGMENT

We thank PShapes project of WoodWisdom.net and Academy of Finland for the financial support.

ABBREVIATIONS

CES	Sodium cellulose ethyl sulfonate
DP	Degree of polymerization
DS	Degree of substitution
WHC	Water holding capacity

REFERENCES

1. T. Trindade and A. Lusa, Biofunctional composites of polysaccharides containing inorganic nanoparticles. in *Advances in Nanocomposite Technology*, A. Hashim (Ed.), Intech – Open Access Publisher, Croatia (2011).
2. T. Heinze, Cellulose: Structure and properties, in *Cellulose Chemistry and Properties: Fibers, Nanocelluloses and Advanced Materials*, O.J. Rojas (Ed.), p. 1, Springer International Publishing, Switzerland (2016).
3. A. Koschella, Synthesis and characterization of branched polysaccharides by reaction of cellulose with 2,3,4,6-tetraacetyl-1-bromo- α -D-glucopyranoside. *Arkivoc.* **2012**(3), 76–89 (2012).

4. M. Gericke, T. Liebert, and T. Heinze, Interaction of ionic liquids with Polysaccharides, 8 – Synthesis of cellulose sulfates suitable for polyelectrolyte complex formation. *Macromol. Biosci.* **9**, 343–353 (2009).
5. T. Ghosh, C. Pujol, E. Damonte, S. Sinha, and B. Ray, Sulfated xylomannans from the red seaweed *Sebdenia polydactyla*: Structural features, chemical modification and antiviral activity. *Antivir. Chem. Chemother.* **19**, 235–242 (2009).
6. M. Kemp and R. Linhardt, Heparin-based nanoparticles. *Wiley Interdiscip. Rev.: Nanomed. Nanobiotechnol.* **2**, 77–87 (2009).
7. L. Balaj, N. Atai, W. Chen, D. Mu, B. Tannous, X. Breakefield, J. Skog, and C.A. Maguire, Heparin affinity purification of extracellular vesicles. *Sci.Rep.* **5**, 10266 (2015).
8. Y. Sakoda, M. Okamatsu, N. Isoda, N. Yamamoto, K. Ozaki, Y. Umeda, S. Aoyama, and H. Kida, Purification of human and avian influenza viruses using cellulose sulfate ester (Cellufine Sulfate) in the process of vaccine production. *Microbiol. Immunol.* **56**, 490–495 (2012).
9. C. He, Z. Yang, and K. Tong, Downstream processing of Vero cell-derived human influenza A virus (H1N1) grown in serum-free medium. *Journal of Chromatography A.* **1218**, 5279–5285 (2011).
10. K. Sugawara, K. Nishiyama, Y. Ishikawa, M. Abe, K. Sonoda, K. Komatsu, Y. Horikawa, K. Takeda, T. Honda, S. Kuzuhara, Y. Kino, H. Mizokami, K. Mizuno, T. Oka, and K. Honda, Development of Vero cell-derived inactivated Japanese encephalitis vaccine. *Biologicals* **30**, 303–314 (2002).
11. A. Sakudo and T. Onodera, Virus capture using anionic polymer-coated magnetic beads (review). *Int. J. Mol. Med.* **30**, 3–7 (2012).
12. H. Dautzenberg, U. Schuldt, G. Grasnack, P. Karle, P. Müller, M. Löhr, M. Pelegrin, M. Piechaczyk, K.V. Rombs, W.H. Günzburg, B. Salmons, and R.M. Saller, Development of cellulose sulfate-based polyelectrolyte complex microcapsules for medical applications. *Ann. N. Y. Acad. Sci.* **875**, 46–63 (1999).
13. K. Lee and D. Mooney, Alginate: Properties and biomedical applications. *Prog. Polym. Sci.* **37**, 106–126 (2012).
14. J. Seppälä, M. Rissanen, and E. Saarikoski, Effect of rheological properties of dissolved cellulose/microfibrillated cellulose blend suspensions on film forming. *Carbohydr. Polym.* **119**, 62–70 (2015).
15. Y. Nishio and T. Ohno, Estimation of miscibility and interaction for cellulose acetate and butyrate blends with N-vinylpyrrolidone copolymers. *Macromol. Chem. Phys.* **208**, 622–634 (2007).
16. Y. Nishio, Y. Teramoto, and K. Sugimura, Blend miscibility of cellulose propionate with poly(n-vinyl pyrrolidone-co-methyl methacrylate). *Carbohydr. Polym.* **98**, 532–541 (2013).
17. M. Pracella, Micro- and nanostructured multiphase polymer blend systems: Phase morphology and interfaces. *Macromol. Chem. Phys.* **208**, 233–233 (2007).
18. R.D. Lundberg and I. Duvdevani, Shear-thickening behavior of ionomers and their complexes, *ACS Symp. Ser.* **462**, 155–175 (1991).
19. Y. Nishio, Y. Teramoto, S. Katano, and K. Sugimura, Cellulose propionate/poly(n-vinyl pyrrolidone-co-vinyl acetate) blends: Dependence of the miscibility on propionyl DS and copolymer composition. *Cellulose* **20**, 239–252 (2012).
20. Y. Nishio, Y. Teramoto, D. Aoki, Y. Miyashita, T. Suzuki, and S. Yoshitake, Nanoincorporation of layered double hydroxides into a miscible blend system of cellulose acetate with poly(acryloyl morpholine). *Carbohydr. Polym.* **93**, 331–338 (2013).
21. J. Trygg and P. Fardim, Enhancement of cellulose dissolution in water-based solvent via ethanol-hydrochloric acid pretreatment. *Cellulose* **18**, 987–994 (2011).
22. L. Gu, J. Yu, F. Li, and S. Zhang, Novel fibers prepared from cellulose in NaOH/thiourea/urea aqueous solution. *Fiber. Polym.* **10**, 34–39 (2009).
23. L. Zhang, Y. Mao, J. Zhou, and J. Cai, Effects of coagulation conditions on the properties of regenerated cellulose films prepared in NaOH/urea aqueous solution. *Ind. Eng. Chem. Res.* **44**, 522–529 (2005).
24. R. Sun, C. Yao, F. Peng, B. Chen, G. Fu, Y. Guan, and S. Zhang, Organic/inorganic superabsorbent hydrogels based on xylan and montmorillonite. *J. Nanomater.* **2014**, 1–11 (2014).
25. P. Sunthar, Polymer rheology, in *Rheology of Complex Fluids*, A.P. Deshpande, J.M. Krishnan, and S. Kumar (Eds.), pp. 171–191, Springer-Verlag, New York (2010).
26. Q. Li, J. Gong, and J. Zhang, Rheological properties and microstructures of hydroxyethyl cellulose/poly(acrylic acid) blend hydrogels. *J. Macromol. Sci. B.* **54**, 1132–1143 (2015).
27. J. Katona, S. Njaradi, V. Sovilj, L. Petrovic, B. Marceta, and J. Milanovic, Rheological properties of hydroxypropylmethyl cellulose/sodium dodecylsulfate mixtures. *J. Serb. Chem. Soc.* **79**, 457–468 (2014).
28. P. Larkin, *Infrared and Raman Spectroscopy; Principles and Spectral Interpretation*, Elsevier Science Publishing Co., Amsterdam (2011).
29. T. Kondo, J. Zhou, J. Cai, L. Zhang, and Y. Mao, Effects of coagulation conditions on properties of multifilament fibers based on dissolution of cellulose in NaOH/urea aqueous solution. *Ind. Eng. Chem. Res.* **47**, 8676–8683 (2008).